

Radar-Based Target Prediction Using SAR and ISAR Imaging

Dipak Mondal

Principal, Kumarganj College, Gour Banga University, West Bengal, India

Abstract Radar-based target prediction plays a crucial role in modern surveillance, reconnaissance, and defense systems. Among various radar technologies, Synthetic Aperture Radar (SAR) and Inverse Synthetic Aperture Radar (ISAR) are widely used for high-resolution imaging and target characterization. These systems provide detailed structural and geometric information about targets under different environmental and operational conditions. However, radar signals are often affected by noise, clutter, motion variations, and signal-to-noise ratio (SNR) fluctuations, leading to uncertainty in prediction. This paper presents an easy-to-understand overview of SAR and ISAR imaging mechanisms, their role in target prediction, associated challenges, and the need for advanced hybrid and uncertainty-aware decision frameworks.

Keywords: SAR, ISAR, target prediction

1. INTRODUCTION

This paper proposes a hybrid radar-based target area prediction combining Synthetic Aperture Radar (SAR) and Inverse Synthetic Aperture Radar (ISAR) imaging approach. High-resolution SAR and ISAR imaging are utilized to extract projected target area. SYSTEMVEU software is used for getting the SAR and ISAR imaging. The Projected target area (Real-time area) is compared with the Theoretical area (given at the time of simulation). Simulation results show a Mean Absolute Error (MAE) of about 266.0 and a Mean Percentage Error (MPE) of 2.22%. The lowest error occurs at a range of 2000 meters, while the highest (4.12%) appears at 200 meters. Variations of Theoretical area and Real time area with Range and Pulse Repetition Interval (PRI) are also studied in this paper. All results reveal a strong consistency between theoretical and real-time area estimations. The scatter plot with a fitted trend line comparing theoretical and real-time areas are also been studied. A trend line equation has also been modelled which shows very weak correlation (-0.21) between Real-time area and Theoretical area which indicates system nonlinearities, calibration offsets, or measurement artifacts affecting real-time results. Radar-based target prediction has evolved significantly over the years. Earlier approaches mainly relied on model-based image formation and feature extraction techniques. Modern systems now integrate data-driven and hybrid approaches to handle the uncertainties present in real-world radar returns.

SAR/ISAR signatures vary strongly with motion and noise, motivating fusion approaches [1-2] that combine multiple features and imaging modalities to increase robustness. Synthetic Aperture Radar (SAR) and Inverse Synthetic Aperture Radar (ISAR) provide complementary image-formation mechanisms. SAR synthesizes fine cross-range resolution through platform motion while ISAR exploits target motion to reveal structural scattering centres making them powerful modalities for high-resolution target description and subsequent prediction tasks. Modern SAR/ISAR processing [3] advances (including hybrid SAR-ISAR pipelines and improved phase-refocusing methods) have increased image fidelity for maritime and airborne scenarios, which in turn improves the stability and discriminability of features used for target-state estimation. SAR/ISAR signatures are often high-dimensional, non-stationary, and corrupted by speckle and motion-induced artifacts, deterministic classifiers alone can struggle with uncertainty and ambiguous

returns; this motivates soft decision frameworks [4]. SAR synthesizes a large aperture by utilizing the motion of the radar platform to generate detailed two-dimensional images of stationary ground scenes, independent of weather and lighting conditions. In contrast, ISAR exploits the relative motion of the target itself such as rotation or vibration to produce high-resolution images of moving objects like ships, aircraft, or vehicles. While both SAR and ISAR provide precise spatial and structural information. Radar measurements often suffer from uncertainties due to noise, clutter, and varying signal-to-noise ratios (SNR).

2. Target detection and area estimation methods

Target detection and area estimation are critical processes in radar-based surveillance and imaging systems. Techniques such as SAR and ISAR play a vital role in generating high-resolution images for identifying and characterizing targets. SAR operates by synthesizing a large antenna aperture through platform motion, enabling detailed imaging of stationary targets over wide areas. ISAR, on the other hand, exploits the relative motion of the target to produce fine-resolution images, making it suitable for moving or rotating objects such as ships or aircraft. However, radar data often contain uncertainties and nonlinear variations due to noise, clutter, and changing environmental conditions.

3. TARGET DETECTION AND AREA ESTIMATION USING SYNTHETIC APERTURE RADAR (SAR) AND INVERSE SYNTHETIC APERTURE RADAR (ISAR) TECHNIQUES

Target detection and area estimation using SAR and ISAR techniques have become essential in modern radar imaging and surveillance systems due to their ability to operate under all hostile conditions. SAR provides high-resolution two-dimensional imagery by synthesizing a large aperture through platform motion, enabling precise detection and mapping of ground or maritime targets based on their backscattering intensity and geometric structure [5-6]. Target area estimation is typically achieved by segmenting the detected regions from SAR images using thresholding, CFAR (Constant False Alarm Rate) algorithms discussed in [7]. ISAR, on the other hand, is particularly effective for detecting and analyzing moving or rotating targets, as it forms two-dimensional images by exploiting the target's motion-induced Doppler frequency variations [8-9]. The combination of SAR and ISAR data enhances both spatial and temporal resolution, allowing accurate estimation of target shape, orientation, and occupied area [10]. Furthermore, recent studies have incorporated feature fusion and adaptive algorithms to integrate range-Doppler and micro-Doppler signatures from ISAR with SAR image features, improving detection reliability and target classification performance under complex clutter conditions [11-12]. Such integrated SAR-ISAR frameworks have shown promise in maritime surveillance, vehicle monitoring, and defense applications, providing robust target detection and area measurement capabilities even in environments with limited visibility or high background interference [13].

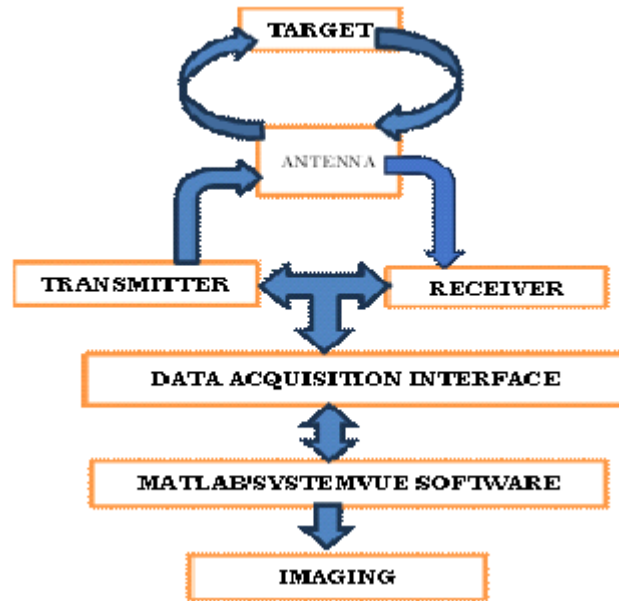


Fig. 1-Technique for detecting targets and estimating area using SAR and ISAR

4. PROTOTYPE OF MEASUREMENT Setup for Target Area Estimation

In this simulation a 5.8 GHz carrier frequency (within the ISM band) is utilized to generate SAR/ISAR radar returns due to its suitable trade-off between range resolution and hardware implementation feasibility. The wavelength at this frequency (~5.17 cm) provides sufficient spatial resolution to accurately extract range and cross-range spreads from the reconstructed radar image. Hence, 5.8 GHz is an effective choice for target area estimation in short-to-medium range imaging scenarios.

Fig.2 shows a prototype of the measurement setup where an aluminum sheet acts as a target which reflects the transmitted electromagnetic waves as returned echoes and are captured by the transceiver RADAR. Both transmitter and receiver interact through a central sound port of laptop (or data acquisition interface), which transfers the digitized radar echoes to the processing environment. The acquired data is then fed into MATLAB/SystemVue software, where signal processing algorithms such as filtering, pulse compression, Doppler estimation, and reconstruction are executed. Finally, the processed data is converted into a visual representation in the imaging block, producing the radar image that reveals the structure, position, or motion characteristics of the target.



Fig 2-Prototype of Measurement setup for SAR/ISAR System

In SAR/ISAR imaging, the estimated cross-range (L_{cr}) and range (L_r) dimensions of the target are obtained from the processed radar image. Range extent is computed from the radar bandwidth B can be expressed as

$$L_r = \frac{c}{2B} \tag{1}$$

where c is the speed of light. The Cross-range extent is determined from the coherent integration time T_i and radar wavelength λ can be written as

$$L_{cr} = \frac{\lambda}{2T_i} \tag{2}$$

After the ISAR/SAR reconstruction, these extents are measured over the pixels of the target region, giving as

$$L_r = (r_2 - r_1)\Delta r, L_{cr} = (\theta_2 - \theta_1)\Delta x \tag{3}$$

where Δr and Δx represent the range and cross-range resolutions. The projected target area (A_t) is then approximated as

$$A_t = L_r \cdot L_{cr} \tag{4}$$

$$A_t = ((r_2 - r_1)\Delta r) \cdot ((\theta_2 - \theta_1)\Delta x) \tag{5}$$

This equation provides a direct geometric estimate of the target's area from the SAR/ISAR reconstructed imagery. Here Table-1 presents the comparison between theoretically assigned and real-time calculated target areas corresponding to different radar ranges and pulse repetition intervals (PRI) at the 5.8 GHz ISM band.

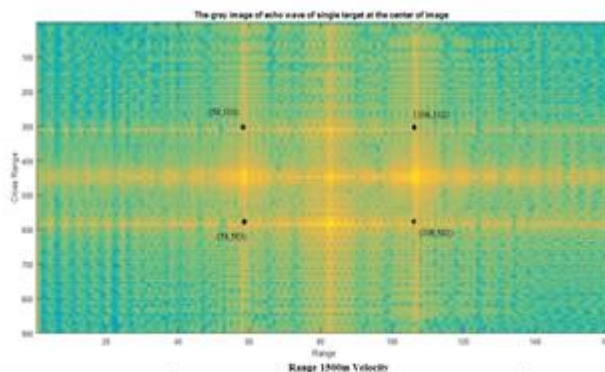


Fig 3-SAR/ISAR image

Fig.3 shows a sample of the real SAR /ISAR image. There are a number of such images from which the results of Table-1 are obtained.

5 ANALYSES OF SIMULATION RESULTS

The results show close agreement between theoretical and simulated values, indicating high consistency in the radar's area estimation accuracy across varying operational ranges. Minor deviations observed may be attributed to environmental noise, signal attenuation, or target motion during real-time measurements. Table-1 below shows the theoretical assigned and real-time calculated areas for each range and PRI value.

TABLE-1: COMPARISON OF THEORETICAL AND CALCULATED REAL TIME TARGET AREAS BY SAR AND ISAR IMAGING TECHNIQUE AT ISM BAND (5.8 GHZ)

Sl. No.	Range (m)	PRI (s)	Area (Theoretical) (sq. units)	Area (Real time) (sq. units)
1	200	0.00500	13,350	12,800
2	500	0.00200	13,258	12,912
3	1000	0.00100	12,960	13,200
4	1500	0.00067	13,008	12,912
5	2000	0.00050	13,104	13,104
6	2500	0.00040	13,056	12,831
7	3000	0.00033	12,864	13,019
8	3500	0.00029	12,960	13,066
9	4000	0.00025	13,584	13,066
10	4500	0.00022	13,056	13,488

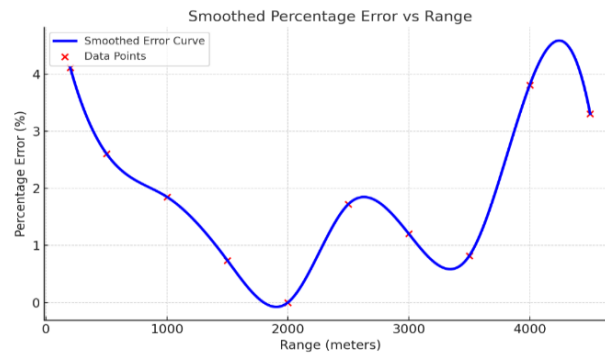


Fig. 4-Percentage Error vs Range plot

Fig.4. shows the error fluctuation across target ranges. Minimal error found around 2000 m and peaks at the shorter range 200 m. The trend clearly shows stable performance in the mid-range region (around 1500–3000 m) with increased deviations at the near and far ranges, indicating edge-range sensitivity in this simulation. Figure-4 shows a Mean Absolute Error (MAE) of approximately 266.0 and a Mean Percentage Error (MPE) of about 2.22%, indicating good overall agreement between theoretical assigned and real-time calculated area. The lowest error occurs at a range of 2000 meters, where the theoretical and real-time values perfectly match, while the highest error of 4.12% is observed at 200 meters. This variation suggests that the radar system performs most accurately at mid-range

distances and experiences slight deviations at shorter ranges, likely due to signal reflections and measurement noise.

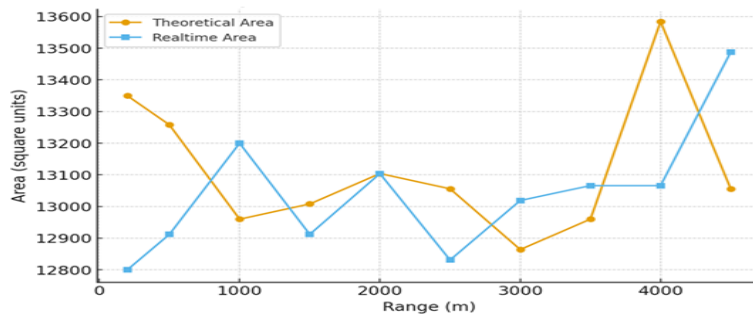


Fig. 5-Variation of Area with Range

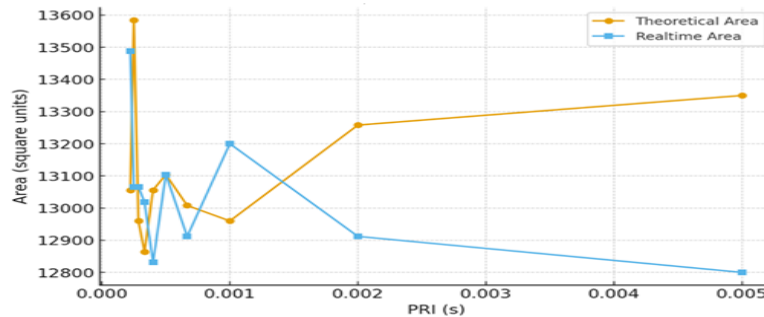


Fig. 6-Variation of Area with PRI

Fig.5 shows the variation of Real time calculated area and Theoretical assigned area with the Range and Fig.6 shows the Real time area and Theoretical area with Pulse Repetition Interval (PRI). From the figures it is observed that both curves generally follow similar trends, with small deviations likely due to real-time measurement noise or system imperfections.

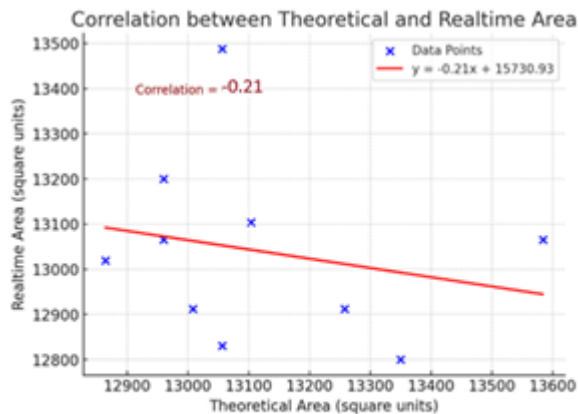


Fig. 7-Correlation between Real time Area with Theoretical area along with Trend line

The scatter plot with a fitted trend line comparing theoretical assigned and real-time calculated areas is shown in Fig.7. It is seen that the data points roughly follow a linear trend, and spread around the line consistent with the weak correlation (-0.21). The fitted linear trend equation can be modelled as

$$\text{Real-time Area} = -0.21 \times (\text{Theoretical Area}) + 15730.93$$

This negative slope suggests an inverse tendency between the datasets, meaning that as theoretical assigned area increases, real-time calculated values slightly decrease overall. Such behaviour may indicate system nonlinearities, calibration offsets, or measurement artifacts affecting real-time results.

6. CONCLUSIONS

This paper is focused on the prediction of the real time area and estimation in percentage error with the theoretical area using the simulation software SystemVue. In this paper hybrid radar-based target prediction approach combining Synthetic Aperture Radar (SAR), Inverse Synthetic Aperture Radar (ISAR) is used. The simulation results show that in the mid band range (1000-3700m) the error is less than 2%. But in the higher and lower range the error becomes higher due to several environmental hazards and measurement inaccuracy. A trend line equation has also been modelled which shows very weak correlation (-0.21) between Real-time area and Theoretical area.

REFERENCES

- [1] J. Deng and F. Su, *Remote Sensing*, 16, 11, p. 1920, (2024).
- [2] Z. Yang, *Remote Sensing*, 12, 13, p. 2077, (2020).
- [3] A. Reigber et al., *DLR, Tech. Rep.* (2013).
- [4] Z. Yan, L. Yu, and Z. Dong, *Sensors*, 20, 7, p. 2037, (2020).
- [5] I. G. Cumming and F. H. Wong, *Digital Processing of Synthetic Aperture Radar Data: Algorithms and Implementation*. Norwood, MA, USA: Artech House, (2005).
- [6] J.M.Lopez-Sanchez and J.Fortuny-Guasch, *IEEE Trans. Antennas Propag.*, 48, 5, 728–737, (2000).
- [7] S. Yu, F. Gao, and L. Zhang, *Inf. Sci.*, 418–419, 601–613, (2017).
- [8] M. Soumekh, *Synthetic Aperture Radar Signal Processing with MATLAB Algorithms*. NewYork, NY, USA: Wiley, (1999).
- [9] Z. Yang et al., *Remote Sensing*, 12, 13, p. 2077, (2020).
- [9] H. Ruan, H. Y. Wu, X. Jia, W. Ye, *IEEE Geosci. Remote Sens. Lett.* 11, 128–132, (2014).
- [10] Z. Yan, Y. Zhang, H. Zhang, *Sensors (Basel)*, 20,7, (2020) Apr 4;20(7):2037. doi: 10.3390/s20072037. PMID: 32260455; PMCID: PMC7180630.

[11] D.Mondal, R.Bera, T.K.Das, &M.Mitra, *Journal of Theoretical and Applied Information Technology*. 37, 1, 22-31, (2012).

[12] Y. Chen et al., *IEEE Geosci. Remote Sens. Lett.*, 19, 1–5, (2022).

[13] H. Wang, Y. Li, and B. Xu, *IEEE Trans. Geosci. Remote Sens.*, 61, 1–13, (2023).